Inter-Channel FWM Mitigation Techniques for 800G-LR4, 1.6T-LR8, 400G-ER4 and 5G Fronthaul Applications Based on O-Band WDM

Xiang Liu, *Fellow, IEEE, Fellow, Optica*, and Qirui Fan

(Invited Paper)

***Abstract*—We review recent advances in the mitigation of inter-channel four-wave-mixing (FWM) based on "XYYX" input polarization alignment, statistical fiber zero-dispersion wavelength (ZDW) distribution, real-world fiber cable installation with randomized fiber ZDW for every fiber segment of typically 2∼3 km during fiber cabling to enable high-performance O-band WDM transmission for 800G-LR4 with four 800 GHz-spaced 200 Gb/s PAM-4 channels reaching up to 10 km, 1.6T-LR8 with eight 800 GHz-spaced 200 Gb/s PAM-4 channels reaching up to 10 km, and 400G-ER4-30 km with four 400 GHz-spaced 100 Gb/s PAM-4 channels reaching up to 30 km. In addition, a novel unequal channel spacing scheme for co-propagating wavelength channels is shown to effectively mitigate the FWM impairment in a bidirectional 5G fronthaul transmission system with twelve 800 GHz-spaced 25 Gb/s NRZ channels reaching up to 20 km. These inter-channel FWM mitigation techniques are expected to aid the standardization of intensity-modulation and direct-detection (IM/DD) based high-speed O-band WDM systems in both IEEE and ITU-T, aiming to cost-effectively and energy-efficiently support future data center, 5G, and metro-access networks.**

***Index Terms*—1.6T-LR8, 400G-ER4, 5G, 800G-LR4, extended reach (ER), four wave mixing (FWM), fronthaul, long reach (LR), O-band, wavelength-division multiplexing (WDM).**

I. Introduction

FOR short-distance data center interconnections and 5G fronthaul links, cost-effective and energy-efficient optical transceivers based on simple intensity-modulation and direct-detection (IM/DD) are commonly used [1]. With the increase of modulation speed to 100Gbaud and beyond, the dispersion tolerance of DD receivers become highly limited. Thus, WDM transmission in the O-band that includes the zero-dispersion wavelength (ZDW) window of standard single-mode fiber (SSMF), i.e., between 1300 nm and 1324 nm, is being considered for both 800Gb/s long-reach (LR) [2] and LAN-WDM based 5G fronthaul transmission [3]. However, inter-channel four-wave-mixing (FWM) was found to impose a severe limitation on the performance of WDM transmission in the O-band [4], [5], [6]. To mitigate the FWM impairment, polarization interleaving [4], [5] and unequal channel spacing [6] had been proposed. More recently, an innovative polarization alignment based on "XYYX" has been proposed [7], [8] and experimentally verified [9] to effectively suppress the FWM impairment in 800G-LR4. In addition, the FWM impairment was shown to be effectively suppressed in a bidirectional 12-channel LAN-WDM fronthaul transmission system (L-WDM) that achieves unequal channel spacing in each direction without scarifying the spectral efficiency [10]. In this article, we substantially extend our OFC 2023 invited article [11], by further considering statistical fiber ZDW distribution [12], and real-world fiber cable installation with randomized fiber ZDW for every fiber segment of typically 2∼3 km during fiber cabling [13], [14], [15], [16] to enable high-performance O-band WDM transmission for the following LR and extended reach (ER) applications:

- 800G-LR4, with four 800 GHz-spaced 200 Gb/s PAM-4 channels reaching up to 10 km,
- 1.6T-LR8, with eight 800 GHz-spaced 200 Gb/s PAM-4 channels reaching up to 10 km,
- 400G-ER4-30 km, with four 400GHz-spaced 100 Gb/s PAM-4 channels reaching up to 30 km.

These inter-channel FWM mitigation techniques are expected to aid the standardization of intensity-modulation and IM/DD based high-speed O-band WDM systems in both IEEE and ITU-T, aiming to cost-effectively and energy-efficiently support future data center, 5G, and metro-access networks.

This article is organized as follows. In Section II, we describe an analytical model to estimate the FWM-induced receiver sensitivity penalty for pulse amplitude modulation 4-level (PAM-4) signals. In Section III, mitigation of inter-channel FWM via the use of "XYYX" polarization arrangement is presented. In Section IV, FWM mitigation due to fiber segmentation induced randomization of fiber ZDW during transmission is described. Section V, the reduction of dispersion penalty due to fiber segmentation is discussed [17]. In Section VI, the combined use of FWM and dispersion mitigation techniques for capacity scaling from 800G-LR4 to 1.6T-LR8 is discussed. In Section VII, the combined use of FWM mitigation techniques, such as the "XYYX" polarization arrangement and ZDW randomization along the fiber link, is shown to enable 400G-ER4

Manuscript received 5 June 2023; revised 14 August 2023 and 8 September 2023; accepted 13 September 2023. Date of publication 15 September 2023; date of current version 2 February 2024. *(Corresponding author: Xiang Liu.)*

The authors are with Huawei Hong Kong Research Center, Hong Kong (e-mail: xiang.john.liu@huawei.com; fan.qirui@huawei.com).

Color versions of one or more figures in this article are available at https://doi.org/10.1109/JLT.2023.3316008.

Digital Object Identifier 10.1109/JLT.2023.3316008

to reach 30 km. Finally, concluding remarks are provided in Section VIII.

II. Inter-Channel FWM Penalty for PAM-4 Signals

FWM is a nonlinear process whereby interactions between three (or two) wavelengths produce one (or two) new wavelengths. FWM is phase-sensitive as its efficiency is strongly affected by phase matching conditions. In WDM transmission over an optical fiber, the strength of the inter-channel FWM effect depends on signal power, fiber nonlinear coefficient, dispersion, dispersion slope, polarization-mode dispersion (PMD), and channel plan w.r.t. the fiber zero dispersion wavelength (ZDW) or zero-dispersion frequency (ZDF) [18], [19]. In the case of four-channel WDM, the worst-case non-degenerate FWM occurs as the ZDW is in the center of four uniformly spaced wavelength channels.

For high-speed data center optics, PAM-4 modulation is becoming the mainstream modulation format. It is worth evaluating the FWM-induced receiver sensitivity penalty in IM/DD systems with PAM-4 modulation. Here, we provide an analytical solution to this problem.

For PAM-4 signal, the uppermost eye is most severely impacted by the signal-crosstalk beat noise. The FWM-induced nonlinear crosstalk (E_{FWM}) on the highest PAM-4 level (E_3) upon intensity (square-law) detection has a standard deviation of

$$\begin{aligned}\sigma_{FWM} &= \mathrm{std}(\alpha \cdot |E_3 + E_{FWM}|^2) \\ &= 2\alpha \cdot |E_3|^2 \cdot \mathrm{std}\left[\mathrm{real}\left(E_{FWM}/|E_3|\right)\right], \end{aligned} \tag{1}$$

where α is a constant related to the conversion from the optical signal E-field to the power level at the receiver decision circuit. The Q-factor corresponding to E_3 without FWM can be expressed as

$$Q_{w/oFWM} = \alpha |E_3|^2 (ER - 1)/ER/6/\sigma_T \tag{2}$$

while the Q-factor corresponding to E_3 with FWM (at an increased received power P'_{RX}) can be expressed as

$$\begin{aligned}Q_{w/FWM} = \alpha |E'_3|^2 (ER - 1)/ER/6/\mathrm{sqrt}[\sigma_T^2 \\ + (P'_{RX}/P_{RX})^2 \sigma_{FWM}^2] \end{aligned} \tag{3}$$

where $|E_3|^2$ and $|E'_3|^2$ are proportional to the received optical power P_{RX} and P'_{RX} in the absence and presence of FWM, respectively, ER is the extinction ratio of the PAM-4 signal, and σ_T^2 is the thermal noise power. Note that the signal-FWM beating noise depends on the received power P'_{RX}, while the thermal noise does not.

For the same target bit error ratio (BER) threshold of BER_0, we have (under the assumption of low BER_0)

$$\begin{aligned}Q_{w/FWM} &= Q_{w/oFWM} = Q_0 \\ &= \mathrm{erfinv}(1 - 2 \cdot 8 \cdot BER_0) \cdot \mathrm{sqrt}(2) \end{aligned} \tag{4}$$

which leads to

$$P'_{RX}/P_{RX} = \mathrm{sqrt}(1 + (P'_{RX}/P_{RX})^2 \cdot \sigma_{FWM}^2/\sigma_{Thermal}^2) \tag{5}$$

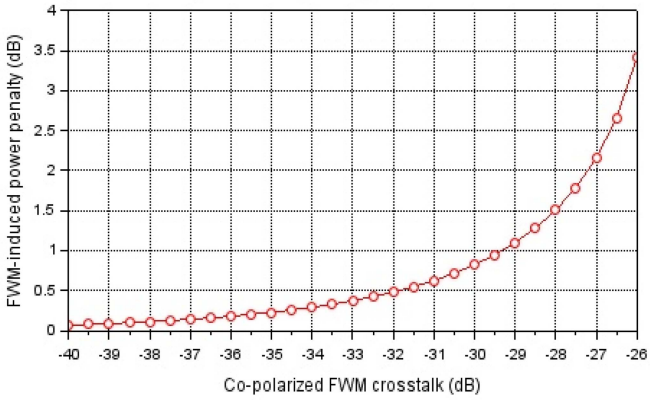

Fig. 1. Calculated FWM-induced receiver sensitivity penalty as a function of co-polarized FWM crosstalk assuming $BER_{th} = 4.85E\text{-}3$ and ER = 5 dB.

After some derivations, we have

$$\begin{aligned}&P'_{RX}/P_{RX} = \\ &\mathrm{sqrt}\{1/[1 - 36 \cdot Q_0^2 \cdot X_{FWM} \cdot ER\,(ER + 1)/(ER - 1)^2]\} \end{aligned} \tag{6}$$

where X_{FWM} is the FWM-induced co-polarized in-band crosstalk power that is normalized to the signal power. Note also that half of the FWM crosstalk is in-phase with the PAM-4 signal and causes the so-called signal-crosstalk beating noise.

Fig. 1 shows the calculated FWM-induced receiver sensitivity penalty as a function of the co-polarized FWM crosstalk assuming a BER_0 of 4.85E-3 and an ER of 5 dB.

For a FWM crosstalk of −33 dB (−30 dB), the FWM-induced receiver sensitivity penalty is 0.4 dB (0.8 dB). These analytical results are in good agreement with the experimental results reported in [20]. In certain LAN-WDM systems, the FWM crosstalk can be higher than -30 dB [4], [5], [6] and needs to be mitigated.

This inter-channel FWM induced transmission impairment in 800G-LR4 has been actively studied by multiple teams within the IEEE 802.3df/dj project [14], [15], [16]. The FWM penalty can be avoided by using statistically significant zero-dispersion wavelength (ZDW) lower limit of 1306 nm, or shifting the laser wavelengths by ∼0.2 nm via slight temperature tuning. The FWM penalty can also be effectively mitigated when using real fiber ZDW distribution [12], as shown in Fig. 2.

The probability density function (PDF) of SSMF ZDW based on data SSMFs from four major fiber suppliers [12] can be approximated as a truncated Gaussian Distribution with a mean of 1313 nm and a standard deviation (std) of 2.2 nm, or $\boldsymbol{N}$(mean = 1313 nm, std = 2.2 nm). When actual fiber cable segmentation is used, a recent analysis shows that the FWM-induced static outage probability (OP) can be reduced to below 1E-7 [16], which will be discussed in the following sections.

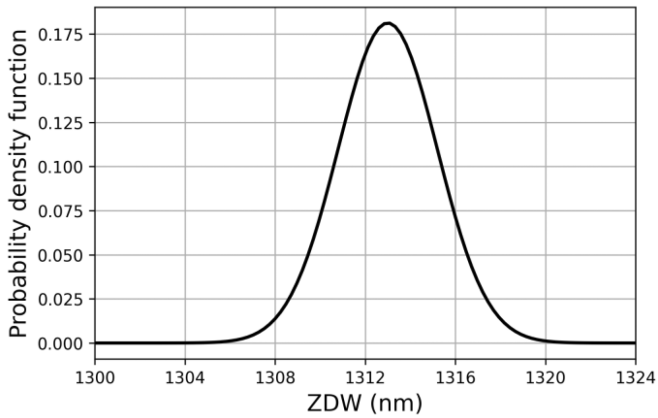

Fig. 2. Probability density function (PDF) of SSMF ZDW based on data SSMFs from four major fiber suppliers (after [12]).

III. Inter-Channel FWM Mitigation via "XYYX" Polarization Arrangement

Fig. 3(a) shows the schematic of an 800G-LR4 IM/DD transceiver with four 224Gb/s PAM-4 channels. The wavelength plan can be based on the longest four wavelengths of LAN-WDM [1], L4∼L7, as shown in Fig. 3(b), or 400GHz-red-shifted [8]. The input polarization alignment of "XYYX" is illustrated in Inset (a). For typical transmission fibers, the random birefringence model (RBM), where the fiber polarization axes and birefringence strength vary randomly with distance, is applicable [18]. Under the RBM, the first three wavelength channels with polarizations "XYY" will not generate any non-degenerate FWM component with X-polarization at the 4th channel under the ideal case of zero PMD, due to this special polarization alignment [19]. Even in the presence of PMD, the phase of the generated FWM component $\varphi_{\mathrm{FWM}}(z) = 2\varphi_{\mathrm{y}}(z)\text{-}\varphi_{\mathrm{x}}(z)$ is fast varying with transmission distance z due to the very short fiber beat length of a few meters typically, so that the phase-matching condition for the non-degenerate "XYYX" FWM interaction is quickly destroyed [8]. Moreover, the degenerate FWM from the two Y-polarized center channels only generates two Y-polarized FWM components at the two edge channel locations, which are orthogonal to the two X-polarized edge channels, so the degenerate FWM induced penalty is also negligibly small [7]. Also, in the three channel WDM case with (XYY) polarization arrangement at frequencies (f_1,f_2,f_3), there is a non-degenerate FWM interaction $f_{1,\mathrm{X}}+f_{3,\mathrm{Y}}\text{-}f_{2,\mathrm{Y}}$ generating $f_{2,\mathrm{X}}$, which is orthogonal with the Y-polarized signal at the same frequency f_2 and thus does not interfere with the signal.

Numerical simulations are performed, using a split-step numerical simulator with the fiber RBM, to quantify the effectiveness of the FWM suppression in LAN-WDM systems. Fig. 4(a) shows the simulated optical spectra after 10-km SSMF transmission with three 800GHz-spaced input signals having "XXX", "YXY", and "XYY" input polarization alignments under zero PMD. Evidently, the FWM interference on the 4th channel in the "XYY" case is the weakest. Fig. 4(b) shows the simulated signal eye diagrams of 224Gb/s PAM-4 signals (with a chirp of 0.5) after 10-km SSMF transmission with four 800GHz-spaced input signals having "XXXX", "XYXY", and "XYYX" input polarization alignments. Consistently, the FWM-induced eye closure is minimized in the "XYYX" case. Fig. 5(a) shows the BER performances for "XXXX", "XYXY", and "XYYX" input polarization alignments under zero PMD and 9 dBm signal launch power per channel, clearly showing the effective FWM suppression in the "XYYX" case. Fig. 5(b) shows the receiver sensitivity penalty at a FEC BER threshold of 4.5×10^{-3} due to dispersion and FWM as a function of the fiber ZDW for the "XYYX" case, indicating unnoticeable FWM penalty for all relevant ZDW values. Fig. 5(c) shows the complementary cumulative distribution function (CCDF) of the FWM penalty with over 2800 fiber PMD realizations, indicating that under the alignment of ZDW and laser frequencies, the FWM-induced "outage" is $\sim 10^{-3}$ for a 1dB penalty and a signal launch power of 5 dBm per channel.

Further assuming that the fiber ZDW distribution is uniform over 1300 nm∼1324 nm, the chance of "FWM wavelength matching" was found to be 0.563% [21]. Due to the laser frequency tolerance of $\Delta f = 100$ GHz, the probability of the FWM being within the receiver bandwidth is approximately $B/2\Delta f$, or 0.56 according to Ref. [5]. Thus, the FWM-induced overall outage probability becomes $\sim 3.2 \times 10^{-6}$ [8], which is reasonably low, given that the PMD-induced outage probability specified in OIF 400ZR is 4.1×10^{-6}. The actual FWM-induced overall outage probability may be much lower when considering (i) the realistic SSMF ZDW distribution [12], [21], (ii) fiber cable splicing induced randomization of ZDW in field-deployed fiber segments that are typically 2∼3 km in length [13], [16], and/or (iii) longitudinal fluctuations of fiber ZDW due to non-uniform fiber fabrication conditions [15], [22].

IV. Inter-Channel FWM Mitigation Due to Fiber Segmentation

It is important to consider the effect of longitudinal ZDW fluctuations along the fiber link in order to avoid overestimation of FWM penalty [15], [22]. As each deployed fiber cable generally consists of multiple cable segments that are spliced together, and the each segment is usually less than 3 km (even for ultra-long-haul systems), as shown in Ref. [13], we need to consider the realistic randomization of ZDW from segment to segment [16]. In this Section, we evaluate the FWM powers for a 10-km G.652 fiber consisting of (i) 2× 5 km (ii) 3× 3.33 km (iii) 4× 2.5 km and (iv) 5× 2 km cable segments where the ZDW is randomized between segments, in comparison with a hypothetic 10-km link without fiber segmentation.

We start with the well-known analysis model describing the FWM power in ZDW region, which is written as

$$P_F\ (f_i, f_j, f_k, \lambda_0, \{L_i\}) = \left(\frac{8}{9}\gamma\frac{D_{ijk}}{3}\right)^2 \frac{P_i(0)\,P_j(0)\,P_k(0)}{A_{eff}^2} e^{-\alpha\left(\sum_1^N L_i\right)}\eta \quad (7)$$

where $P_i(0)$, $P_j(0)$, $P_k(0)$ are the input powers of f_i, f_j, f_k frequencies, P_F is the FWM power at $f_F = f_i + f_j - f_k$; α, γ,

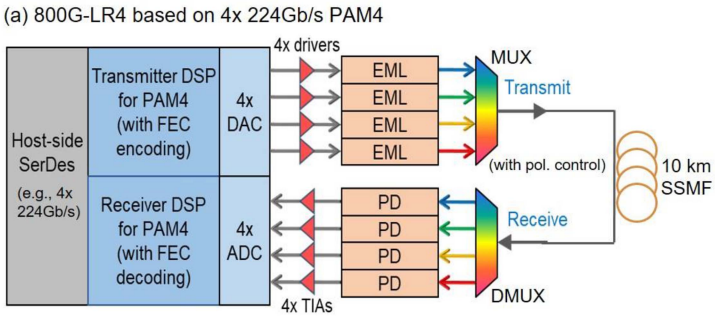

(b) Four LAN-WDM wavelengths in or near the ZDW window

LAN-WDM index	Center frequency (THz)	Center wavelength (nm)	Dispersion after 10km (ps/nm)
L4	231.4	1295.56	-26.16 ~ -4.08
L5	230.6	1300.05	-22.03 ~ 0.05
L6	229.8	1304.58	-17.87 ~ 4.21
L7	229.0	1309.14	-13.67 ~ 8.41

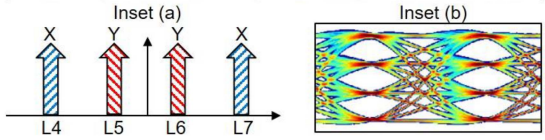

Fig. 3. (a) Schematic of an 800G-LR4 IM/DD transceiver with four 224 Gb/s PAM-4 channels; (b) A wavelength plan based on LAN-WDM. Inset (a): Illustration of the "XYYX" input polarization alignment. Inset (b): An exemplary eye diagram of a 224 Gb/s PAM-4 signal.

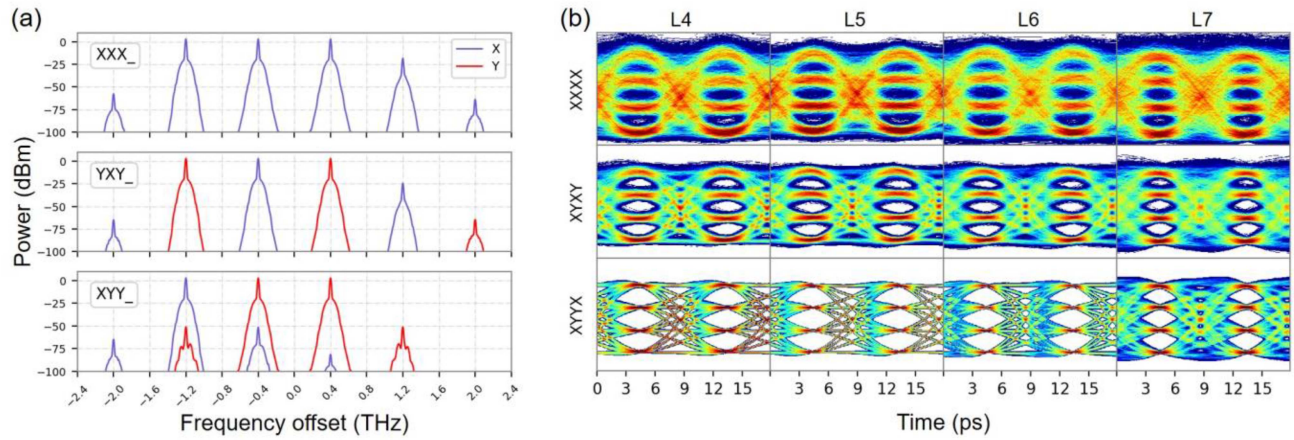

Fig. 4. (a) Simulated optical spectra after 10-km SSMF transmission with three 800GHz-spaced input signals having "XXX", "YXY", and "XYY" input polarization alignments; (b) simulated signal eye diagrams after 10-km SSMF transmission with four 800 GHz-spaced input signals having "XXXX", "XYXY", and "XYYX" input polarization alignments. Simulation model: RBM for PMD = 0; launch power per channel: 6 dBm; fiber ZDF: 230.2 THz.

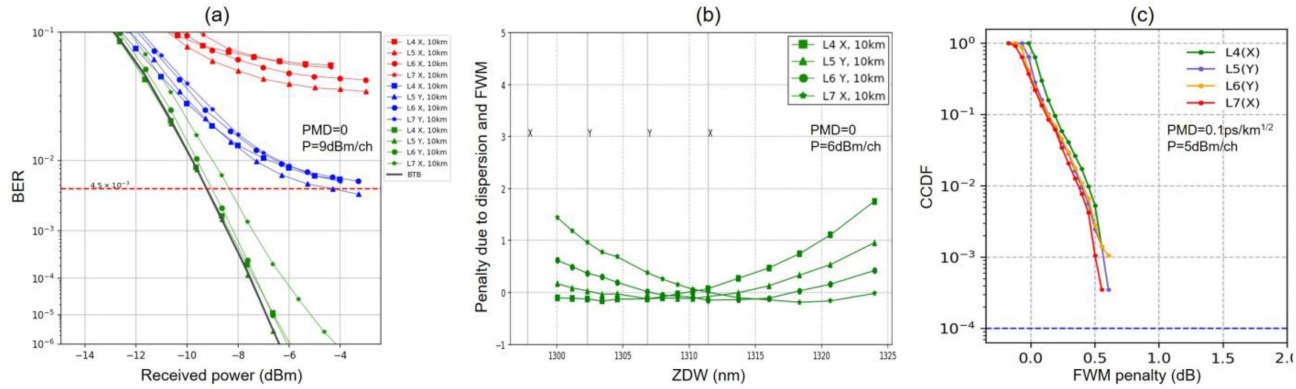

Fig. 5. (a) Simulated BER performance after 10-km SSMF transmission for "XXXX", "XYXY", and "XYYX" input polarization alignments; (b) the receiver sensitivity penalty due to dispersion and FWM as a function of the fiber ZDW for the "XYYX" case; and (c) CCDF of the simulated FWM penalty with over 2800 PMD realizations. Fiber ZDF: 230.2 THz, exactly at the center of the four LAN-WDM channels, L4, L5, L6, and L7.

D_{ijk}, and A_{eff}^2 denote fiber loss, nonlinear coefficient, degeneracy factor and fiber effective area around ZDW λ_0, respectively; L_i denotes the length of the *i-th* segment of the fiber link, and η is the FWM efficiency as a function of phase-mismatch $\Delta\beta$. By considering boundary conditions between consecutive fiber segments, η was extended to 2-segment case having independent ZDW's [18]. Following the same approach, it is straightforward to further generalize η to multi-sectional cases, which has a

TABLE I
SIMULATION PARAMETERS USED FOR 800G-LR4

Parameters	Values
L4 ($\lambda 0$)	1295.56 nm
L5 ($\lambda 1$)	1300.06 nm
L6 ($\lambda 2$)	1304.59 nm
L7 ($\lambda 3$)	1309.14 nm
Fiber effective area	70 μm^2
Fiber nonlinear reflective index	2.6E-20 m^2/W
CD slope	0.09 ps/(nm^2·km)
Fiber attenuation	0.31 dB/km
Launch power	5.65 dBm/channel
PMD coefficient	0 ps/sqrt(km)

compact form

$$\eta = \left| \sum_{i=1}^{N} \prod_{j=1}^{i-1} e^{(-\alpha + i\Delta\beta_j)L_j} \frac{e^{(-\alpha+i\Delta\beta_i)L_i} - 1}{i\Delta\beta_i - \alpha} \right|^2 \quad (8)$$

The total received P_F at f_F given λ_0, simply denoted as $\sum P_F(f_F)|_{\lambda_0}$, is the n-segment accumulation of the sum of P_F over all $\{i, j, k\}$ combinations, assuming FWM tones of same frequencies can be coherently combined. In fact, such assumption may be too strong as each $\{i, j, k\}$ light field was suggested to have uniformly distributed random phase in practice [23], rendering lower total FWM crosstalk. The ratio of received total FWM power and channel launch power at f_F frequency is referred as the XPM crosstalk for that channel. With this iterative technique, we can evaluate XPM crosstalk in probabilistic manner by randomizing λ_0. Using Monte-Carlo simulations, we have assessed the FWM crosstalk (X_{FWM}) distributions under the assumption that the 10-km LR link consists of multiple fiber segments with random ZDW values within the ZDW distribution shown in Fig. 2.

Totally, 100 million ZDW realizations have been performed with the key simulation parameters specified in Table I. Each channel has launch power of 5.6 dBm, and worst-case polarization alignment ("XXXX" with PMD = 0) is considered where the four channels are exactly uniformly spaced.

Fig. 6. Shows the simulated CCDF of FWM crosstalk after 800G-LR4 transmission over 10-km SSMF link consisting of a single 10-km segment with the ZDW distribution shown in Fig. 2. From the results, we can see that the probability of having FWM crosstalk, defined here as the generated FWM power (P_{FWM}) divided by the signal launch power (P_I), larger than −30 dB is about 4E-5, indicating noticeable FWM penalty.

Fig. 7 shows the simulated CCDF of FWM crosstalk after 800G-LR4 transmission over a 10-km SSMF link consisting of five 2-km segments with independent ZDW's. From the results, we can see that the probability of having X_{FWM} larger than −33.5 dB is as low as 1E-7. Further considering realistic channel misalignments and raw BER averaging over 4 channels, the effective FWM crosstalk at 1E-7 static OP is <-34.5 dB, indicating practically insignificant penalty.

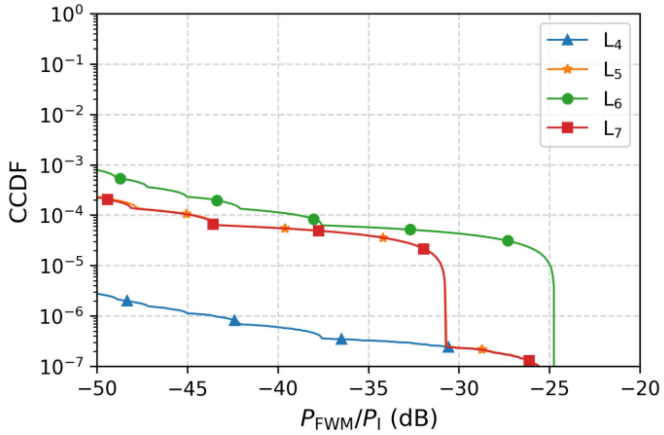

Fig. 6. Simulated CCDF of FWM crosstalk after 800G-LR4 transmission over 10-km SSMF link consisting of a single 10-km segment with a fixed ZDW.

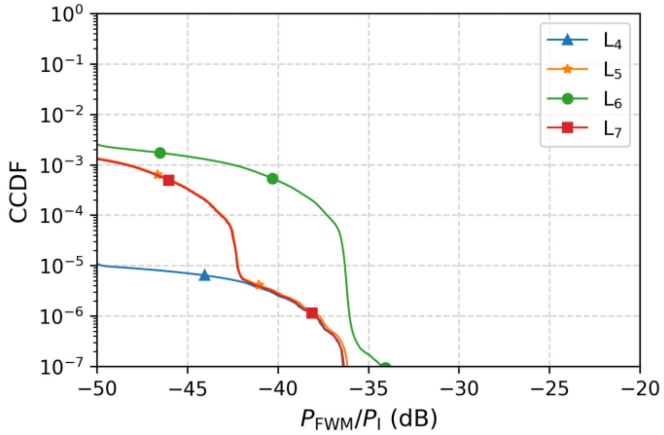

Fig. 7. CCDF of FWM crosstalk after 800G-LR4 transmission over a 10-km SSMF link consisting of five 2-km segments with independent ZDW's.

With the further consideration of the "effect of longitudinal ZDW fluctuation" within each cable segment [15], [22], the FWM penalty is expected to further reduced. In addition, field-deployed systems are operating with extra margin, because of statistical distribution of component and fiber losses and impairments, therefore the actual static OP is even lower. Given the above, the 800G-LR4 baseline specification proposed in Ref. [21] is expected to be well supported in real-world deployments [16], especially when the "XYYX" FWM suppression technique is also utilized as well.

V. DISPERSION PENALTY REDUCTION DUE TO FIBER SEGMENTATION

In the specification of IEEE 800G-LR4 optical modules, the ZDW values for the PAM-4 transmitter and dispersion eye closure penalty (TDECQ) measurements are recently proposed to be different from the worst-case SSMF ZDW values, i.e., 1300 nm and 1324 nm, in order to minimize the overall system cost [24]. The two ZDW values under consideration for TDECQ measurements are $ZDW_1 = 1305$ nm and $ZDW_2 = 1319$ nm,

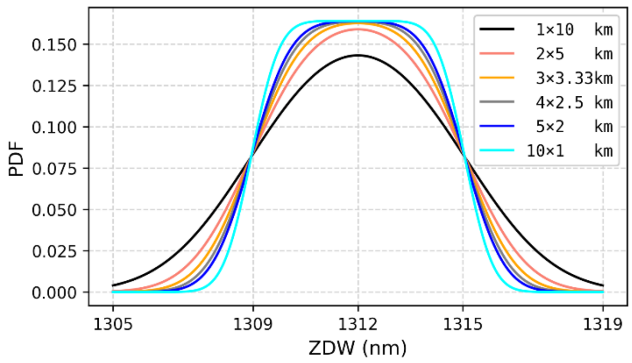

Fig. 8. PDF of the 10-km ZDW_{link} under the assumptions of 1, 2, 3, 4, 5 and 10 segments in the link.

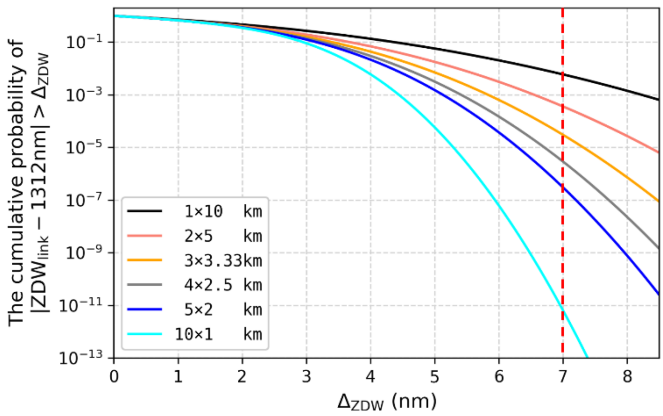

Fig. 9. Cumulative probability of the 10-km ZDW_{link} being outside a given range under the assumptions of 1, 2, 3, 4, 5 and 10 segments in the link.

based on a statistical model [24]. This statistical model assumes a normal distribution having a standard deviation (σ) of 2nm, and a mean value (ZDW_{mean}) that is uniformly distributed from 1309 to 1315 nm for each fiber segment, i.e., $N(ZDW_{mean} = 1309\sim1315$ nm, $\sigma = 2$ nm), which accounts for variation among fiber manufacturers and mean shifts [24]. In this Section, we show that the probability of CD penalty higher than that predicted by TDECQ measurement at 1305 and 1319 nm (P_{CD}) is very low (e.g., <1E-6) when actual fiber cable segmentation is taken into consideration in a rigorous analysis [17]. To evaluate the PDF of the LR link ZDW's, we assume that

- The fiber cable segments in a given 10-km link when they happen to come from the same manufacturing batch are correlated and have a fixed ZDW_{mean} that is inside [1309 nm, 1315 nm], which is on the conservative side), and
- The distribution of ZDW_{mean} inside [1309 nm, 1315 nm] is uniform, which is also on the conservative side.

The resulting PDF's of the LR link ZDW's under the assumptions of 1, 2, 3, 4, 5 and 10 segments in the 10-km link are shown in Fig. 8.

Fig. 9 shows the probability for the ZDW of the entire 10-km link (ZDW_{link}) being outside the [1305 nm, 1319 nm] window in a 10-km SSMF fiber link consisting of (i) 2 × 5 km, (ii) 3 × 3.33 km, (iii) 4 × 2.5 km, (iv) 5 × 2 km, and (v) 10 × 1 km cable segments, as compared to that in a hypothetic 10 km link without cable segmentation. The region to the right of the red dashed line indicates ZDW_{link} being outside [1305 nm, 1319 nm], corresponding to a deviation from the mean (Δ_{ZDW}) of 7 nm.

From Fig. 9, it can be seen that the probability of CD penalty higher than that predicted by TDECQ measurement at 1305 and 1319 nm is very low (e.g., <1E-6) when actual fiber cable segmentation with the assumption that the ZDW is randomized between segments is taken into consideration. Field-deployed systems are operating with extra margin, because of statistical distribution of component and fiber losses and impairments, therefore the actual P_{CD} is even lower. Thus, the two ZDW test points proposed in Ref. [24] represent statistically significant worst-case dispersion scenarios. Given the above, the "SMF Channel Specification Proposal Using Existing ITU-T Codes" [24] for link budget calculations and transceiver testing is well supported. In effect, this statistical approach to specify the chromatic dispersion (CD) penalty is similar to that specifying the PMD_Q in multiple ITU-T standards recommendations [25], and a specification on a new CD_Q parameter can be developed in the future [26], [27].

TABLE II
CHANNEL WAVELENGTH PLAN OPTIONS FOR 1.6T-LR8

Option 1 (400-GHz spacing without G)	Option 2 (400-GHz spacing with G)	Option 3 (800-GHz spacing without G)	Option 4 (800-GHz spacing with G)
1293.32 (X)	1291.10 (X)	1277.89 (X)	1273.54 (X), L0
1295.56 (Y)	1293.32 (Y)	1282.26 (Y)	1277.89 (Y), L1
1297.80 (Y)	1295.56 (Y)	1286.66 (Y)	1282.26 (Y), L2
1300.05 (X)	1297.80 (X)	1291.10 (X)	1286.66 (X), L3
1302.31 (X)	1300.05 (G)	1295.56 (X)	1291.10 (G), L_G
1304.58 (Y)	1302.31 (X)	1300.05 (Y)	1295.56 (X), L4
1306.85 (Y)	1304.58 (Y)	1304.58 (Y)	1300.05 (Y), L5
1309.14 (X)	1306.85 (Y)	1309.14 (X)	1304.58 (Y), L6
	1309.14 (X)		1309.14 (X), L7

Note: the wavelengths listed in this table is in units of nm.

VI. SCALING CAPACITY FROM 800G-LR4 TO 1.6T-LR8

With the FWM impairment being effectively suppressed by using the "XYYX" polarization arrangement and/or reducing the ZDW_{link} region (e.g., to 1305 nm∼1319 nm), it is feasible to scale up the transceiver capacity to 1.6 Tb/s via eight wavelength channels. Table II shows four options of channel and polarization arrangements for 1.6T-LR8. In Option 1, eight 400 GHz-spaced 224 Gb/s PAM-4 channels with "XYYXXYYX" input polarization alignment may be used [7]. In Option 2, a guard band (G) of 400 GHz may be added in the middle of the eight wavelength channels [15], so the channel plan become "XYYXGXYYX". For cost-effective implementations, it is preferred that four of the eight wavelength channels are located on the LAN-WDM's 800-GHz grid.

When the ZDW_{link} region is reduced as discussed in Section V, the dispersion penalty is reduced and it is feasible for 1.6T-LR8 to leverage the widely used LAN-WDM wavelengths

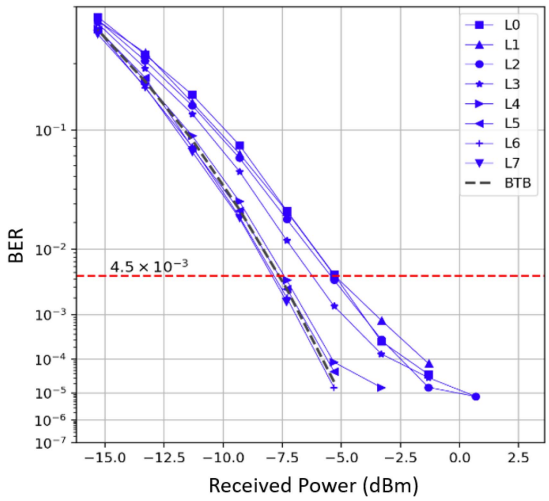

Fig. 10. Simulated receiver sensitivity of 1.6T-LR8 after 10 km SSMF transmission. MLSE is applied in the receiver signal processing.

with 800-GHz spacing to be more cost-effective. In Option 3, all the channels are spaced at 800 GHz without a guard band. In Option 4, the original eight-channel LAN-WDM wavelength plan is used, where an 800 GHz guard band is added in the middle of the eight channels (L_G) to facilitate easy multiplexing/demultiplexing of the 800G-LR4 band (L4∼L7) with/from the newly added four channels.

Fig. 10 shows the simulated receiver sensitivity performances of all the LR8 channels for Option 4 (800-GHz spacing with G) after 10-km SSMF transmission at the ZDW test point of 1319 nm, which represents the worst-case CD penalty. In the simulations, maximum-likelihood sequence estimation (MLSE) is applied in the receiver signal processing to improve the CD tolerance. At a BER threshold of 4.5E-3, all the eight channels achieve a receiver sensitivity of better than −5 dBm and a TDECQ of less than 2 dB, which are sufficient to meet the LR link budget as in the case of LR4 [21].

VII. Extending Reach From LR to ER

In some data center and metro network applications, extending the reach beyond LR is needed. The 100G Lambda multi-source agreement (MSA) group [28] has recently developed the 400G-ER4-30 km specification based on four 400GHz-spaced 106.25-GB/s PAM-4 channels, centered at 1304.58 nm, 1306.85 nm, 1309.14 nm and 1311.43 nm, for reaching 30 km in SSMF. As the FWM impairment is more severe in the 400G-ER4-30 km case than that in the 800G-LR4 case, we need to use the "XYYX" based FWM suppression technique, and carefully consider the impact of the link PMD that may reduce the effectiveness of the "XYYX" technique.

To evaluate FWM crosstalk subject to the link PMD, a direct approach is full field simulation, which however can hardly allow us to extract FWM at signal frequency. Instead, we introduced a simplified simulation technique assuming fiber birefringence does not depend on channel loading. Specifically, 3 CW channels (λ0-2) and 1 CW channel (λ3) are transmitted separately over a pair of identical optical fiber links (with same PMD randomizations), referred as probe link and reference link respectively; at the output of probe link, FWM field, extracted by an optical filter centered at λ3, can be divided into its co-polarized and orthogonal components with respect to the received state of polarization (SoP) of λ3 CW of reference link. The ratio of co-polarized and λ3 in terms of their measured power is referred as the FWM crosstalk of interest. Note that this CW FWM may be a slight overestimate since different bit patterns in neighboring channels help to statistically reduce FWM crosstalk in practice.

With this fast simulation geared toward this specific interest, we conduct 1000000 PMD realizations (10000 fiber realizations × 100 input SoP) within reasonable time. Besides the parameters already given as above, the extra fiber parameters related to Split-Step Fourier Method (SSFM) solver are listed in Table III.

The simulation results are summarized in Figs. 11, 12, and 13. The key takeaway messages are:

1) As compared to the worst-case polarization alignment (i.e., "XXXX" with PMD = 0), "XYYX" suppresses the "co-polarized" FWM power by over 10 dB for PMD < 0.09ps/sqrt(km) at a static OP of 10% (Fig. 11), or for PMD < 0.05ps/sqrt(km) at a static OP of 1% (Fig. 12).

TABLE III
Simulation Parameters for Assessing the Effectiveness of the "XYYX" FWM Suppression Technique in the Presence of PMD

Parameters	Values
RMB	On
Correlation Length	20m
PMD Step width	200m
Split Fourier Step maximal phase change	0.05 degree
Number of PMD coarse step realizations	10,000
Number of Input SoP realizations	100

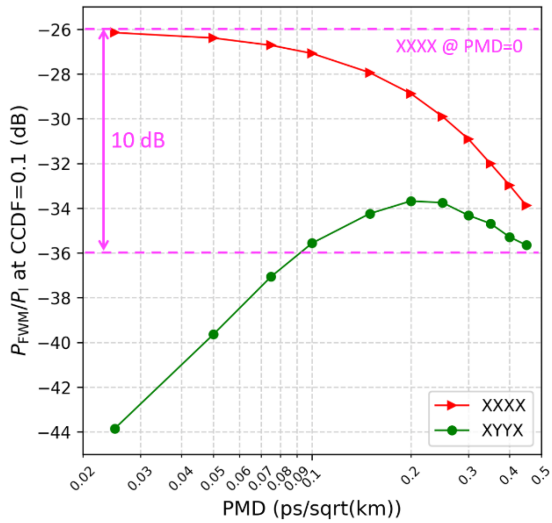

Fig. 11. FWM crosstalk at CCDF = 0.1 for 400G-ER4-30 km transmission under the "XXXX" and "XYYX" polarization arrangements for different link PMD coefficients. P_{launch} = 5.8 dBm/channel, ER = 5 dB.

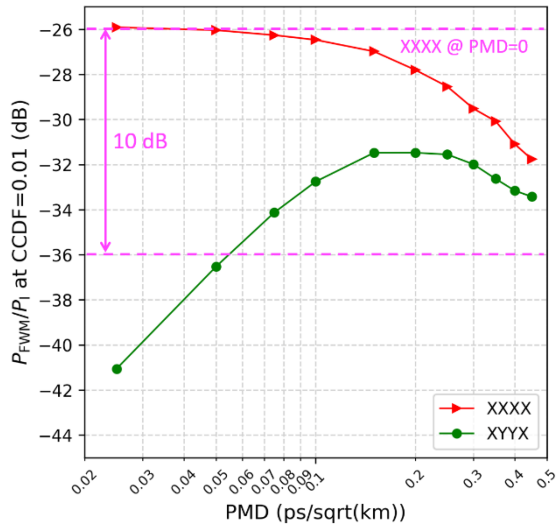

Fig. 12. FWM crosstalk at $CCDF = 0.01$ for 400G-ER4-30 km transmission under the "XXXX" and "XYYX" polarization arrangements for different link PMD coefficients. $P_{launch} = 5.8$ dBm/channel, ER = 5 dB.

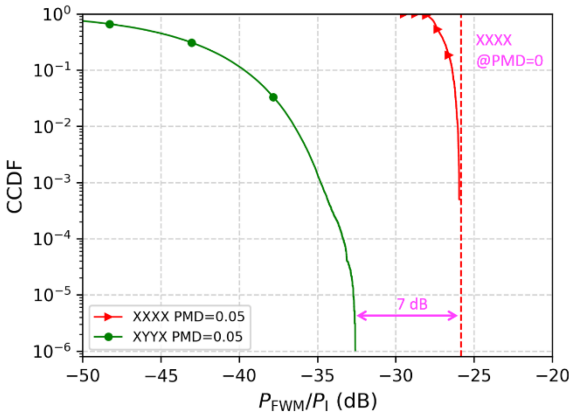

Fig. 13. CCDF of the FWM crosstalk for 400G-ER4-30 km transmission under the "XXXX" and "XYYX" polarization arrangements when the link PMD is 0.05 ps/sqrt(km). $P_{launch} = 5.8$ dBm/channel, ER = 5 dB.

2) For a static OP of 1E-6, "XYYX" suppresses the FWM crosstalk by 7 dB as compared to the worst-case polarization alignment (i.e., "XXXX" with PMD = 0).

We then conduct Monte-Carlo simulations for the worst-case polarization alignment (i.e., "XXXX" with PMD = 0) with the additional consideration of realistic fiber segmentation in fiber cable deployments. The 30-km ER link is assumed to consist of ten 3-km fiber segments whose ZDW's are independent. The ZDW of each fiber segment follows the Gaussian distribution presented in Ref. [12]. Totally, over 100 million link realizations are simulated. Fig. 14 shows the CCDF of FWM crosstalk after 400G-ER4-30 km transmission over a 30-km SSMF link consisting of ten 3-km segments with independent ZDW's.

For the "XXXX" case, at the static outage probability of 1E-7, the FWM crosstalk is about −28 dB. For the "XYYX" case, the FWM crosstalk would be suppressed by 7 dB to about −35 dB based on the results shown in Fig. 13. Such a low FWM

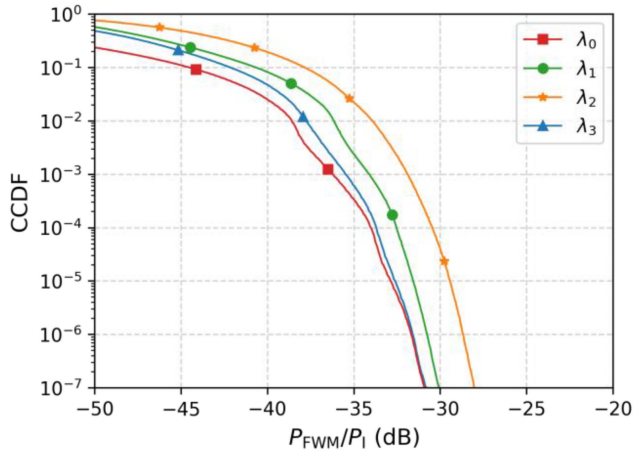

Fig. 14. Simulated CCDF of FWM crosstalk after 400G-ER4-30 km transmission over a 30-km SSMF link consisting of ten 3-km segments with independent ZDW's. $P_I = 5.8$ dBm/channel. ER = 5 dB.

crosstalk would cause a small penalty of less than 0.4 dB. It is worth noting that when the worst-case FWM occurs when the link ZDW is in the middle of the four wavelength channels, at which the CD penalties for the four ER4 channels are minimized and are typically lower than the maximum CD penalty by over 1 dB. Thus, when considering the transmission penalty from the combined effects of CD and FWM, there is no need to allocate an extra penalty for FWM beyond what is already allocated for the maximum CD penalty. With the combined use of the "XYYX" FWM suppression technique and fiber segmentation induced ZDW randomization along the fiber link, 400G-ER4-30 km has been supported with sufficient margin [28].

VIII. 5G Fronthaul Based on Bidirectional O-Band WDM Transmission With 800-GHz Channel Spacing

For short-distance 5G C-RAN front-haul links, low-cost optical transceivers based on IM/DD are usually used, together with widely-installed G.652 fibers. With IM/DD, fiber dispersion effect cannot be fully compensated as in the case of digital coherent optical detection, thus the low-dispersion O-band is well suited. The ITU-T is working on a work item termed G.owdm for "Multichannel bi-directional WDM applications with single-channel optical interfaces in the O-band" [3]. In this work item, a 12-channel L-WDM approach based on 25-Gb/s non-return-to-zero (NRZ) optical transceivers is be actively evaluated. It leverages the ecosystem for LAN-WDM and expands the number wavelength channels from eight (in LAN-WDM) to twelve as shown in Fig. 15.

Due to the acceleration of 5G C-RAN construction and the rapid growth of intra-data-center transceivers using O-band optics, the ecosystem of the O-band WDM system is fast growing. It is expected that the O-band WDM network will expand from front-haul to the metro-access segment. The next-generation O-band WDM technology can be considered in terms of WDM bandwidth, channel data rate, and channel spacing. In terms of WDM bandwidth, the existing 12-channel L-WDM front-haul solution supports further expansion. However, the

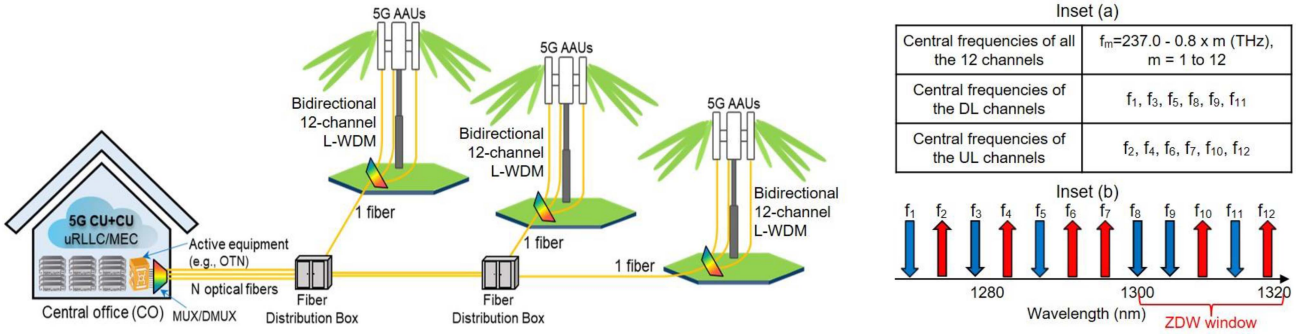

Fig. 15. Illustration of a 5G fronthaul transmission system that uses a single fiber to connect each cell site via bidirectional 12-channel L-WDM. Inset (a): The center frequencies of the downlink (DL) and the uplink (UL) wavelength channels. Inset (b): Illustration of the unequal channel spacing for both the DL and the UL wavelength channels in the ZDW window of the SSMF.

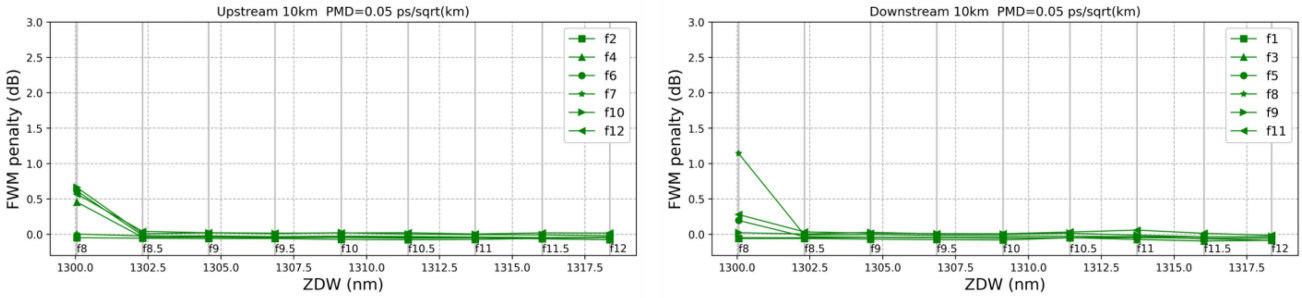

Fig. 16. Simulated receiver sensitivity penalty at BER=5×10^{-5} due to FWM vs. the fiber ZDW. Signal launch power: 5.5 dBm/channel.

up-scaling solution will face performance deterioration at long wavelengths due to dispersion. In terms of channel rate, doubling the per-channel data rate from 25 Gb/s to 50 Gb/s by using PAM-4 modulation is feasible. In terms of channel spacing, the current channel spacing of 800 GHz may be reduced to 400/200/100 GHz, and provide 2/4/8 times more wavelength channels. One transmission issue that needs to be further studied is the FWM-induced nonlinear penalties on wavelength channels that are close to the fiber ZDW.

Fig. 15 illustrates a 5G fronthaul transmission system that uses a single fiber to connect each cell site via bidirectional 12-channel L-WDM [1]. Bidirectional transmission makes it easy to realize accurate synchronization, which is required for 5G fronthaul [1]. We can take the advantage of the bidirectional transmission property to realize unequal channel spacing in each direction to effectively mitigate FWM. With the use of unequal channel spacing in the ZDW window for each of the DL and UL directions, as shown in Insets (a) and (b), the FWM penalty can be effectively suppressed [10], [11].

Fig. 16 shows that the receiver sensitivity penalties due to FWM for all the relevant fiber ZDW values are smaller than the allocated optical path penalty of 2 dB [10], [11].

Fig. 17 shows a "black link" approach for bi-directional applications with two fibers connecting to each transceiver in accordance with G.owdm [3] where the head-end equipment (HEE) to tail-end equipment (TEE) direction uses the UL wavelength channel plan shown in Fig. 15, while the TEE-to-HEE direction uses the DL wavelength channel plan shown in Fig. 15, to mitigate the FWM impairments in both directions.

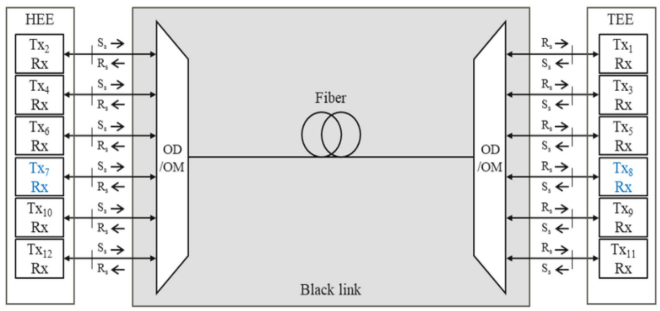

Fig. 17. Linear "black link" approach for bi-directional applications with two fibers connecting to each transceiver in accordance with G.owdm [3].

IX. Conclusion

We have reviewed recent advances in mitigating the inter-channel FWM impairments for O-band WDM based 800G-LR4, 1.6T-LR8, 400G-ER4-30km, and bidirectional 5G fronthaul with twelve 800GH-spaced channels. With the effective mitigation of the FWM impairments, IM/DD will continue to be a viable technology for cost-effectively and energy-efficiently supporting future high-speed data center, 5G, and metro-access networks.

ACKNOWLEDGMENT

The authors wish to thank many colleagues working in the IEEE 802.3df/dj 800G-LR4 project for stimulating discussions. Among them are Rang-Chen (Ryan) Yu, Ernest Muhigana, Nobuhiko Kikuchi, Frank Chang, John Johnson, Chris Cole, Maxim Kuschnerov, and Roberto Rodes.

REFERENCES

[1] X. Liu, *Optical Communications in the 5G Era*. New York, NY, USA: Academic, 2021.
[2] "IEEE P802.3df 200 Gb/s, 400 Gb/s, 800 Gb/s, and 1.6 Tb/s ethernet task force," 2023. [Online]. Available: https://www.ieee802.org/3/df/public/index.html
[3] ITU-T Work Item G.owdm on, "Multichannel bi-directional WDM applications with single-channel optical interfaces in the O-band."
[4] X. Liu, C. McKinstrie, N. Cheng, and F. Effenberger, "Suppression of Four-Wave-Mixing (FWM) for 100G-EPON," Contribution liuxiang_3ca_1a_0517, IEEE 802.3ca Meeting, May 2017.
[5] J. Johnson, "FWM Analysis of PAM-4 LR/ER PMDs," Contribution johnson_3df_optx_01_220414, IEEE 802.3df Meeting, Apr. 2022.
[6] R. Rodes, V. Bhatt, and C. Cole, "On Technical Feasibility of 800G-LR4 with Direct-Detection," Contribution rodes_3df_01a_220329, IEEE 802.3df Meeting, Mar. 2022.
[7] X. Liu, Q. Fan, T. Gui, K. Huang, and F. Chang, "Effective Suppression of Inter-Channel FWM for 800G-LR4 and 1.6T-LR8 Based on 200Gb/s PAM-4 Channels," Contribution liu_3df_01b_2207, IEEE 802.3df Meeting, Jul. 2022.
[8] X. Liu et al., "Assessment of the Combined Penalty from FWM and Dispersion in 800G-LR4 Based on 224Gb/s PAM-4," Contribution liu_3df_01a_221012, IEEE 802.3df Meeting, Oct. 2022.
[9] D. Lewis, S. Tanaka, and N. Kikuchi, "Experimental Verification of Polarization Multiplexing for Suppressing FWM," Contribution lewis_3df_01_221012, IEEE 802.3df Meeting, Oct. 2022.
[10] H. Liu et al., "Updated Proposal for G.owdm Specifications," Contribution T22-SG15-C-0025, ITU-T SG Plenary, Sep. 2022.
[11] X. Liu and Q. Fan, "Inter-channel FWM mitigation techniques for O-band WDM based 800G/1.6T LR and 5G Fronthaul applications," in *Proc. Opt. Fiber Commun. Conf. Exhib.*, 2023, pp. 1–3.
[12] C. Cole et al., "Update to Modern SMF Parameters for Calculating PMD (Physical Medium Dependent) Penalties," Contribution cole_3df_01a_2211, IEEE 802.3df Meeting, Nov. 2022.
[13] C. Zhang et al., "Optical layer impairments and their mitigation in C+L+S+E+O multi-band optical networks with G.652 and loss-minimized G.654 fibers," *J. Lightw. Technol.*, vol. 40, no. 11, pp. 3415–3424, Jun. 2022.
[14] M. Kuschnerov, Y. Lin, T. Yu, and N. Stojanovic, "Further Discussion of DGD Penalty and Specification for 800G LR4," Contribution kuschnerov_3df_01a_2211, IEEE 802.3df Meeting, Nov. 2022.
[15] E. Muhigana, S. Tanaka, and N. Kikuchi, "Numerical Simulation of Polarization Multiplexing for Suppressing FWM," Contribution kikuchi_3dj_01b_230206, IEEE 802.3dj Meeting, Feb. 2023.
[16] X. Liu et al., "Rigorous 800G-LR4 FWM Suppression Analysis using Actual Fiber Cable Segmentation," Contribution liu_3dj_01_2303, IEEE 802.3dj Meeting, Mar. 2023.
[17] X. Liu et al., "Probability of CD Penalty Higher than that Predicted by TDECQ Measurement at 1305 and 1319nm," Contribution liu_3dj_01_230, IEEE 802.3dj Meeting, Mar. 2023.
[18] K. Inoue, "Polarization effect on four-wave mixing efficiency in a single-mode fiber," *IEEE J. Quantum Electron.*, vol. 28, no. 4, pp. 883–894, Apr. 1992.
[19] C. J. McKinstrie, H. Kogelnik, R. M. Jopson, S. Radic, and A. V. Kanaev, "Four-wave mixing in fibers with random birefringence," *Opt. Exp.*, vol. 12, pp. 2033–2055, 2004.
[20] M. Kuschnerov, T. Rahman, Y. Lin, and J. Zheng, "Update on Component and Channel Characterization for Optical 200G PAM4," Contribution kuschnerov_3df_02a_221012, IEEE 802.3df Meeting, Oct. 2022.
[21] R. Rodes et al., "Towards an 800G-LR4 IMDD Specification Consensus - May 2023 Update," Contribution rodes_3dj_01_2305, IEEE 802.3dj Meeting, May 2023.
[22] E. Myslivets, N. Alic, J. R. Windmiller, and S. Radic, "A new class of high-resolution measurements of arbitrary-dispersion fibers: Localization of four-photon mixing process," *J. Lightw. Technol.*, vol. 27, no. 3, pp. 364–375, Feb. 2009.
[23] G. P. Agarwal, *Lightwave Technology: Telecommunication Systems*. Hoboken, NJ, USA: Wiley, 2005.
[24] C. Cole, "SMF Channel Specification Proposal Using Existing ITU-T Codes," Contribution cole_3dj_01_230516, IEEE 802.3dj Meeting, May 2023.
[25] See, for example, ITU-T Recommendations G.652, G.653, G.654, G.655 and G.656.
[26] V. Ferretti and A. Lambert, "802.3dj SMF Channel Definition CDq Approach Utilizing PMDQ Methodology," Contribution to the IEEE 802.3dj ad-hoc meeting, Jun. 2023.
[27] X. Liu et al., "Baseline CDq values for 800GBASE-LR4," Contribution liu_3dj_01a_2307, IEEE 802.3dj Meeting, Jul. 2023.
[28] "400G-ER4-30 technical specification 1.0, by the100G Lambda MSA Group," 2023. [Online]. Available: https://100glambda.com/specifications/summary/2-specifications/12-400g-er4-30-technical-specification-1-0

Xiang Liu (Fellow, IEEE) received the Ph.D. degree in applied physics from Cornell University, Ithaca, NY, USA, in 2000. He is currently the Chief Expert of optical communications standards with Huawei Technologies. He has more than 20 years of working experience in optical communications. He has authored more than 350 publications and holds more than 100 U.S. patents. He is the author of a book entitled *Optical Communications in the 5G Era*, and a Fellow of OSA (now OPTICA). His research interests include optical communication technologies, systems, and networks. He was the General Co-Chair of OFC 2018, and is currently the Deputy Editor of *Optics Express*.

Qirui Fan received the B.Eng. and M.Sc. degrees in communication engineering from Hunan University, Changsha, China, in 2014 and 2017, respectively, and the Ph.D. degree in optical fiber communications from The Hong Kong Polytechnic University, Hong Kong, in 2022. Since 2022, he has been with the Huawei Technologies as a Researcher of optical communications standards. His research interests mainly include advanced signal processing, simulation technologies, and systems optimizations for optical communications.